

VIP

## A Strategy for Neuraminidase Inhibitors Using Mechanism-Based Labeling Information

Hiroshi Hinou,<sup>\*,[a]</sup> Risho Miyoshi,<sup>[a]</sup> Yasuaki Takasu,<sup>[a]</sup> Hirokazu Kai,<sup>[a]</sup>  
 Masaki Kuroguchi,<sup>[a]</sup> Shingo Arioka,<sup>[b]</sup> Xiao-Dong Gao,<sup>[a]</sup> Nobuaki Miura,<sup>[a]</sup>  
 Naoki Fujitani,<sup>[a]</sup> Shinya Omoto,<sup>[c]</sup> Tomokazu Yoshinaga,<sup>[c]</sup> Tamio Fujiwara,<sup>[c]</sup>  
 Takeshi Noshi,<sup>[b]</sup> Hiroko Togame,<sup>[b]</sup> Hiroshi Takemoto,<sup>[b]</sup> and Shin-Ichiro Nishimura<sup>\*,[a]</sup>

**Abstract:** A potent inhibitor for *Vibrio cholerae* neuraminidase (VCNA) was developed by using a novel two-step strategy, a target amino acid validation using mechanism-based labeling information, and a potent inhibitor search using a focused library. The labeling information suggested the hidden dynamics of a loop structure of VCNA, which can be a potential target of the novel inhibitor. A focused library composed of 187 compounds was prepared from a 9-azide derivative of 2,3-dehydro-*N*-

acetylneuraminic acid (DANA) to interrupt the function of the loop of the labeled residues. Inhibitor **3c** showed potent inhibition properties and was the strongest inhibitor with FANA, a *N*-trifluoroacetyl derivative of DANA. Validation studies of the inhibitor with a detergent and a Lineweaver–Burk

plot suggested that the 9-substitution group would interact hydrophobically with the target loop moiety, adding a noncompetitive inhibition property to the DANA skeleton. This information enabled us to design compound **4** having the combined structure of **3c** and FANA. Compound **4** showed the most potent inhibition ( $K_i = 73$  nM, mixed inhibition) of VCNA with high selectivity among the tested viral, bacterial, and mammal neuraminidases.

**Keywords:** drug design • hydrolases • inhibitors • sialic acid • structure–activity relationship

### Introduction

Neuraminidases (NAs; EC 3.2.1.18)—a family of glycoside hydrolase enzymes that cleave the glycosidic linkages of sialic acid (Neu5Ac; neuraminic acid) located on the surface

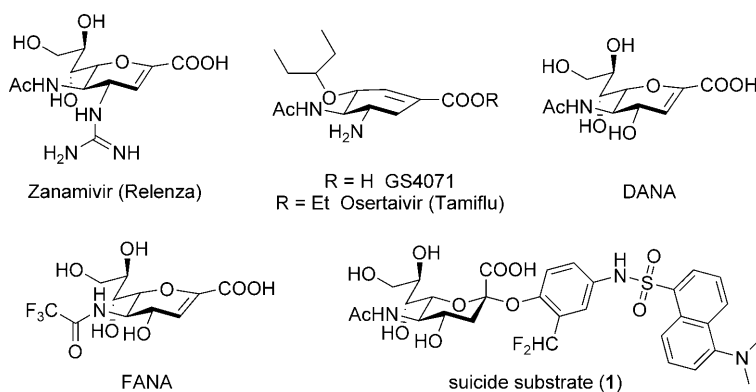
of glycoproteins and the cells of vertebrates—regulate interactions with the extracellular world including infection, immunity, and cell–cell adhesion.<sup>[1]</sup> In particular, many pathogens, such as viruses, bacteria, and protozoa, utilize their own NAs for invasion, nutrition, detachment, and immunologic escape.<sup>[2]</sup> Thus, NA inhibitors are an attractive target for drug discovery. *Vibrio cholerae* neuraminidase (VCNA), the oldest and best studied NA,<sup>[3]</sup> is involved in cholera pathogenesis by degrading the mucin layer of the gastrointestinal tract to enhance the attachment of the bacteria by trimming higher-order gangliosides to GM1, a putative receptor of the cholera toxin,<sup>[4]</sup> and catabolizing Neu5Ac.<sup>[5]</sup> A structural study of VCNA revealed that this enzyme has two lectin-like domains other than the central catalytic domain, and alignment of the active site is very similar to that observed in influenza (Flu) NA and *Salmonella* NA.<sup>[6]</sup> Despite the success of the “structure-based inhibitor design”<sup>[7]</sup> for production of anti-influenza drugs such as zanamivir (Relenza)<sup>[8]</sup> and oseltamivir (Tamiflu; ethyl ester of GS4071),<sup>[9]</sup> an inhibitor design for VCNA lacks the ability to surpass the nonselective NA inhibitor 2,3-dehydro-2-deoxy-*N*-acetylneuraminic acid (DANA) and its *N*-trifluoromethyl deriva-

[a] Dr. H. Hinou, R. Miyoshi, Y. Takasu, H. Kai, Dr. M. Kuroguchi, Dr. X.-D. Gao, Dr. N. Miura, Dr. N. Fujitani, Prof. S.-I. Nishimura  
 Graduate School of Life Science and Frontier Research  
 Center for the Post-Genome Science and Technology  
 Hokkaido University  
 N21, W11, Kita-ku, Sapporo 001-0021 (Japan)  
 Fax: (+81)11-707-9042  
 E-mail: hinou@glyco.sci.hokudai.ac.jp

[b] Dr. S. Arioka, Dr. T. Noshi, Dr. H. Togame, Prof. H. Takemoto  
 Shionogi Innovation Center for Drug Discovery  
 Shionogi & Co., Ltd.  
 N21, W11, Kita-ku, Sapporo 001-0021 (Japan)

[c] Dr. S. Omoto, Dr. T. Yoshinaga, Dr. T. Fujiwara  
 Discovery Research Laboratories  
 Shionogi & Co., Ltd., 5-1, Mishima 2-Chome  
 Settsu, Osaka 566-0022 (Japan)

Supporting information for this article is available on the WWW under <http://dx.doi.org/10.1002/asia.201000594>.



Scheme 1. Reported neuraminidase inhibitors.

tives (FANA, Scheme 1),<sup>[10]</sup> which were reported in 1974.<sup>[11]</sup> Conformational flexibility of the loop moieties in the catalytic site of the NA<sup>[12,13]</sup> might be a novel target for the design of potent and selective VCNA inhibitors because the active site of the NAs is mainly composed of amino acid residues on a loop moiety in the  $\beta$ -propeller-type catalytic domain,<sup>[6]</sup> and the conformational change in the loop moiety is involved in the catalytic mechanism (Figure 1a). Chavas et al.<sup>[12]</sup> demonstrated in crystallographic studies that the human cytosolic NA (Neu2) has two flexible loops containing Glu111 and catalytic Asp46 residues, which are disordered in the apo form but ordered with DANA to adapt two short  $\alpha$  helices to cover the inhibitor and locate Asp46 for catalysis. Russell et al.<sup>[13]</sup> demonstrated that the influenza virus NAs (N1–N9) could be classified into two structurally distinct groups by conformational changes in the so-called “150-loop”, which contains the catalytic Asp151 residue. Group 1 is composed of the N1, N4, N5, and N8 subtypes with an additional cavity adjacent to their active sites relative to group 2 (N2, N3, N6, N7, and N9). Despite this information, only one FluNA inhibitor recognized the structural change in the 150-loop<sup>[14]</sup> by sacrifice of the affinity of the zanamivir skeleton because such a dynamic target is not suitable for design based only on static structural information. We thought that mechanism-based labeling of these flexible loops<sup>[15]</sup> could predict the dynamic nature with

actual affinity information and design a new inhibitor of the loop moiety.

Previously, we reported a mechanism-based labeling study of VCNA by using 2-difluoromethylaryl<sup>[16]</sup> sialoside **1**<sup>[17]</sup> (Scheme 1), and following protease digestion, separation of the labeled peptide fragment using an anti-dansyl column. MALDI-TOF/TOF MS analysis revealed that the Asp576 and Arg577 residues located in a peripheral hydrophobic loop (<sup>575</sup>LDRFFL<sup>580</sup>) in the

catalytic domain were labeled by the aglycone of **1** (Figure 1a).<sup>[17]</sup> The two labeled sites indicate that this enzyme is active after the first aglycone **1** attack but is inactive after the second attack. Interestingly, crystallographic data (PDB: 1W0O)<sup>[18]</sup> of VCNA indicated that the two amino acid residues are about 20 Å away from the anomeric position of NeuAc in the active-site pocket covered with a loop (<sup>246</sup>VGGGDPGALSN<sup>256</sup>), which includes a putative catalytic Asp251 residue; the Asp576 residue is buried within the catalytic domain, and the consecutive phenylalanine residues next to the labeled sites are exposed to the composed hydrophobic surface on VCNA (Figure 1b). This suggested that the labeled residues are located on the hydrophobic flexible loop, and that the Asp576 and Arg577 residues appear to interact with the aglycone of **1** after hydrophobic recognition corresponding to the catalytic action of VCNA. Although the crystallographic data of VCNA with DANA (PDB: 1W0O) and the apo form (PDB: 1W0P) did not show the dynamism (Figure 1c)<sup>[18]</sup> that occurs with human neuraminidase 2 (*h*Neu2)<sup>[12]</sup> and FluNA,<sup>[13]</sup> the hydrophobic loop 575–580 and an intermediate large loop (<sup>312</sup>PTDAAQNGDRIKPWMP<sup>327</sup>) lying between the hydrophobic loop and DANA were not conformationally stabilized<sup>[6,18]</sup> (Figure 1a). Thus, we designed potent and specific inhibitors based on the labeling information, hydrophobic affinity, and putative dynamism of the loop structures. In this paper, we describe a novel strategy for neuraminidase inhibitors by using the information of mechanism-based labeling and a focused library designed by validation of the labeling mechanism.

### Abstract in Japanese:

シアリダーゼは感染や生体恒常性に密接に関わる加水分解酵素であり、創薬標的となりうる。我々はコレラ症に関与するコレラシアリダーゼ(VCNA)を標的とし、自殺基質による標識位置情報と結晶構造から基質認識における未知の動的機構を予測した。その予測に基づき、遷移状態基質モデルであるデヒドロシアル酸 (DANA) 骨格を有するフォーカスライブラリを作成し、新奇阻害剤 **3c** を見出した。**3c** は最強の既知 VCNA 阻害剤である N-TFA 化 DANA 誘導体 (FANA) に匹敵する阻害強度と、極めて高い VCNA 選択性を示した。さらに、**3c** と FANA はその修飾による相互作用点が全く異なることから双方の特徴を有する FANA 誘導体 **4** を作成したところ、より高い阻害能( $K_i = 73 \text{ nM}$ )と高選択性を示した。

## Results and Discussion

### Design and Synthesis of a Focused Library for the Inhibition of VCNA

To design the novel inhibitor skeleton for VCNA, the following four points were considered: 1) the ring skeleton of DANA interacts with the strictly conserved amino acid residues among the NAs; 2) the 9-position of DANA is directed to the labeled loop; 3) the steric barrier of an intermediate

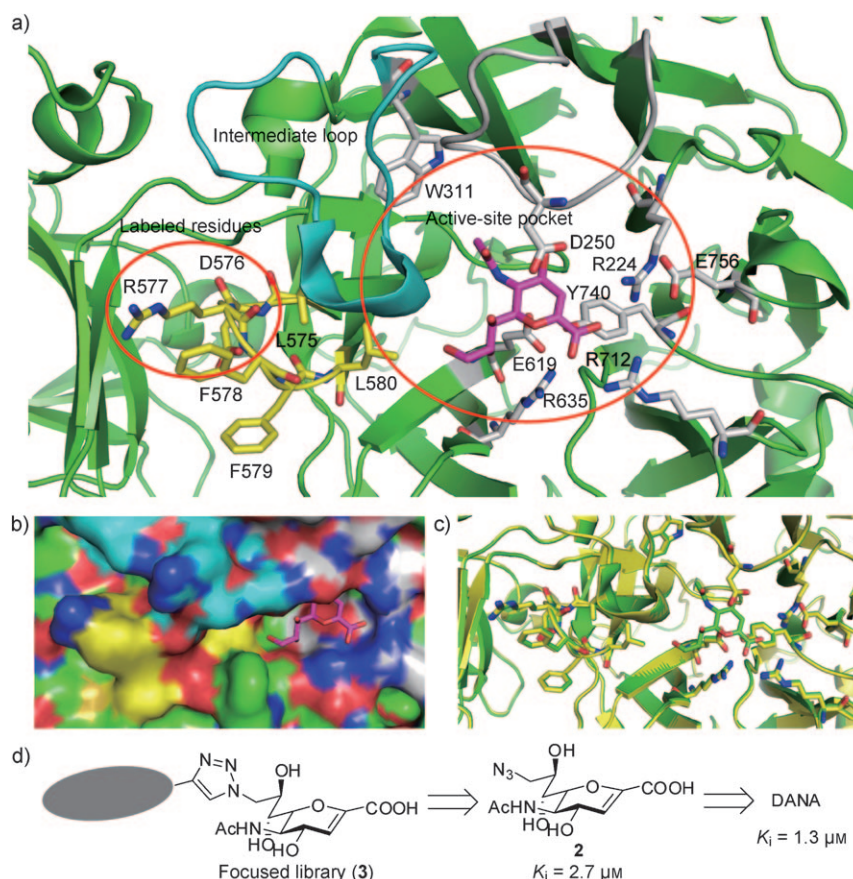


Figure 1. Structural analysis of VCNA (PDB ID 1W00) active site: a) the catalytic domain of VCNA [DANA (pink); conserved residues (W311, D250, E619, Y740, E756, R224, R635, R712) and catalytic loop <sup>246</sup>VGGGDPGALS<sup>N256</sup> (gray), intermediate large loop <sup>312</sup>PTDAAQNGDRIKPWMP<sup>327</sup> (light blue), labeled residues by **1** (D576 and R577), and hydrophobic loop <sup>575</sup>LDRFFL<sup>580</sup> (yellow)]; b) surface model of VCNA active site in which the ligand was placed in the deep pocket of the active site and the catalytic loop and the intermediate loop must move away to open the pocket for the ligand recognition; c) superposition of the VCNA–DANA complex (green, PDB ID 1W00) and an apo VCNA (yellow, PDB ID 1W0P). Clear structural changes cannot be found from these structures; d) inhibitor design based on the mechanism-based labeling information.

large loop from Pro312 to Pro327 (Figure 1a) can be ignored because this loop moves away from DANA during the recognition process; and 4) the hydrophobic surface of the labeled loop moves toward DANA and the distance is variable. Based on these four considerations, a focused library **3** with a modification point at the C9 position of the DANA skeleton was designed. The random structure at the C9 position of library **3** was constructed by a [2+3] cyclization (click reaction)<sup>[19]</sup> between the azide group of 9-azide-9-deoxy-DANA **2**<sup>[20]</sup> with the terminal alkyne group of a commercially available compound library (Figure 1d).

### Screening From the Focused Library

For the first screening, the alkyne compounds (266 compounds) were coupled with **2** in a uniform click reaction.<sup>[19]</sup> The efficiency of each [2+3] cyclization reaction for **3** was roughly estimated by ESI-TOF MS without any purification, and 187 reaction mixtures with a ratio of intensity greater

than 70% for product **3** versus **2** were used for the screening of the VCNA inhibition activity (see the Supporting Information). The triazole derivatives **3** (100 μM; calculated as the click reactions 100% yield) were incubated with 2- $\alpha$ -(4'-methylumbelliferyl)-*N*-acetylneuraminic acid (4-MU-NANA; 2 mM) and VCNA (0.15 mU; Figure 2a). The reagents used for the click reaction (copper ion, etc.) did not inhibit the VCNA activity (Figure 2b). We classified each compound into five groups based on the relative remaining activity in the screening result, and eight compounds (**3a–h**; each structure is shown in the Supporting Information) that belonged to the most potent group (0–0.2 relative activity) were selected for the second screening (Figure 2a). The eight compounds were prepared again as purified compounds, and 50 μM of each compound was incubated again with 4-MU-NANA (1 mM) and VCNA (0.45 mU) for a second screening. Three compounds (**3a**, **3c**, and **3d**) showed the significantly potent inhibition of VCNA (78, 95, and 88% inhibition activity, respectively), whereas DANA showed only a 12% inhibition (Figure 2c).

### Validation of the Inhibition Mode of **3a**, **3c**, and **3d**

The order of the inhibition strength in the second screening changed from the order in the first screening (**3f** > **3c** > **3e** > **3g** > **3h** > **3a** > **3d** > **3b**) and each selected compound (**3a**, **3c**, and **3d**) with an amphiphilic structure was suspected to form an aggregate and act as a promiscuous inhibitor.<sup>[21]</sup> To validate the inhibition mode of compounds **3a**, **3c**, and **3d**, the influence of the detergent Triton-X100 on inhibition strength and concentrations of the inhibitors<sup>[22]</sup> was determined (Figure 3). The reserved structure of the sigmoid curve after addition of detergent (0, 0.01, and 0.1%) clearly showed that all three compounds interacted with VCNA in a 1:1 ratio. Among these three compounds, **3c** and **3d** had a slight shift in the sigmoid curve, which suggested weakening of the inhibition property by the addition of the detergent. This suggested that an independent hydrophobic interaction was involved in the binding of VCNA and **3c** (and **3d**) as a

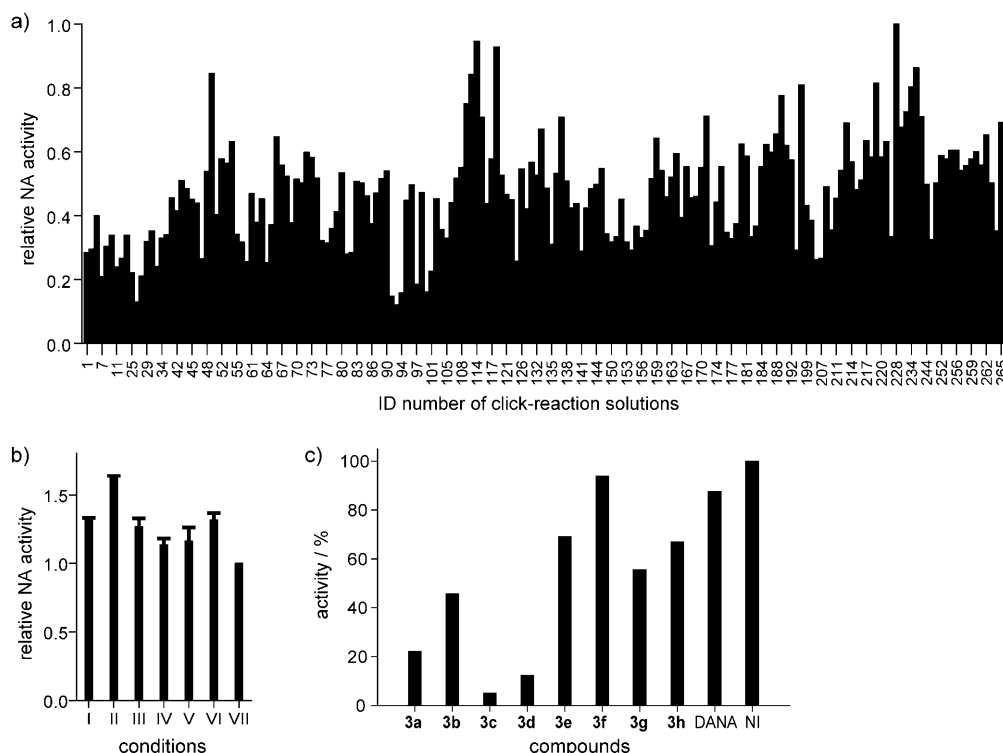


Figure 2. Screening results of the focused library: a) result of the first screening for VCNA (0.15 mU) with substrate (2 mM) and click-reaction solutions from 100  $\mu\text{M}$  of **2** and alkyne compounds; b) effect of the reagents for click reactions towards VCNA activity: I) DMSO, II) *t*BuOH/H<sub>2</sub>O, III) Cu<sup>2+</sup>, IV) ascorbate, V) TBTA, VI) mixture of I–V, VII) blank; c) second screening for VCNA (0.15 mU) with substrate (1 mM) and purified compounds **3a–h** (50  $\mu\text{M}$ ), and DANA. NI=no inhibitor.

source of inhibition potency. The dissociation constant for inhibitor binding ( $K_i$ ) values of DANA, FANA, **3a**, **3c**, and **3d** were determined from the Lineweaver–Burk (LB) plots as 1.3, 0.15, 1.4, 0.22, and 0.52  $\mu\text{M}$ , respectively. The LB plot showed that **3c** and **3d** exhibited a mixed inhibition mode compared to that of DANA and FANA, which showed a clear competitive inhibition mode (Figure 3). The detergent-based assay and LB plot suggested that **3c** and **3d** bind the catalytic site of VCNA with the DANA skeleton to provide competitive inhibition, and the hydrophobic biphenyl moiety presumably interacts with the hydrophobic loop <sup>575</sup>LDRFFL<sup>580</sup> and is attributed with providing a noncompetitive inhibition mode.

The specificity of **3c** for VCNA among the various neuraminidases is also of great interest to validate our strategy. DANA, FANA, and **3c** were assayed for influenza B virus NA (FluB NA) and human neuraminidase 2 (*h*Neu2) as viral and mammal neuraminidases, respectively. As shown in Table 1, **3c** showed a high specificity for VCNA among the three tested neuraminidases. The  $K_m/K_i$  ratios ( $K_m$ =Michaelis–Menten constant) of **3c** and FANA for VCNA were almost the same, but the ratios for FluB NA and *h*Neu2 were completely different. In the case of FluB NA, the N-substitution from DANA to FANA affords half  $K_i$  values, and the 9-substituent group from DANA to **3c** affords more than 1000 times greater  $K_i$  values. In the case of *h*Neu2, each substitution resulted in a similar shift of  $K_i$  values as

Table 1.  $K_m$  [ $\mu\text{M}$ ] values of 4-MU-NANA and  $K_i$  [ $\mu\text{M}$ ] values of DANA, FANA, **3a**, **3c**, and **3d** for viral, microbial, protozoal, and mammal neuraminidases.

Compounds	VCNA	FluB NA	<i>h</i> Neu2
4-MU-NANA	41	10	540
DANA	1.3 [32] <sup>[a]</sup>	0.93 [11] <sup>[a]</sup>	114 [4.7] <sup>[a]</sup>
9-N <sub>3</sub> DANA ( <b>2</b> )	2.7 [15] <sup>[a]</sup>	–	–
<b>3a</b>	1.4 [29] <sup>[a]</sup>	–	–
<b>3c</b>	0.22 [186] <sup>[a]</sup>	>1000 [ $<0.01$ ] <sup>[a]</sup>	501 [1.1] <sup>[a]</sup>
<b>3d</b>	0.52 [79] <sup>[a]</sup>	–	–
FANA	0.15 [273] <sup>[a]</sup>	0.33 [30] <sup>[a]</sup>	43 [13] <sup>[a]</sup>

[a]  $K_m/K_i$  ratios are shown in brackets.

FluB NA ( $1/3$  and 5 times the  $K_i$  values, respectively). This suggests that the *N*-trifluoroacetyl group interacts with hydrophobic amino acid residues that are structurally stabilized by  $\beta$ -sheet formation among the NAs (W311, W101, and I103 residues in VCNA, FluB NA, and *h*Neu2, respectively) to nonselectively enhance the affinity. On the other hand, the 9-substituent group of **3c** specifically interacts with the “movable” hydrophobic loop of VCNA to enhance affinity but repulses the corresponding position in FluB NA and *h*Neu2.

#### Design, Preparation, and Evaluation of **4**

The independent interaction of the 9-substitution group of **3c** and the *N*-trifluoroacetyl group of FANA suggests that a

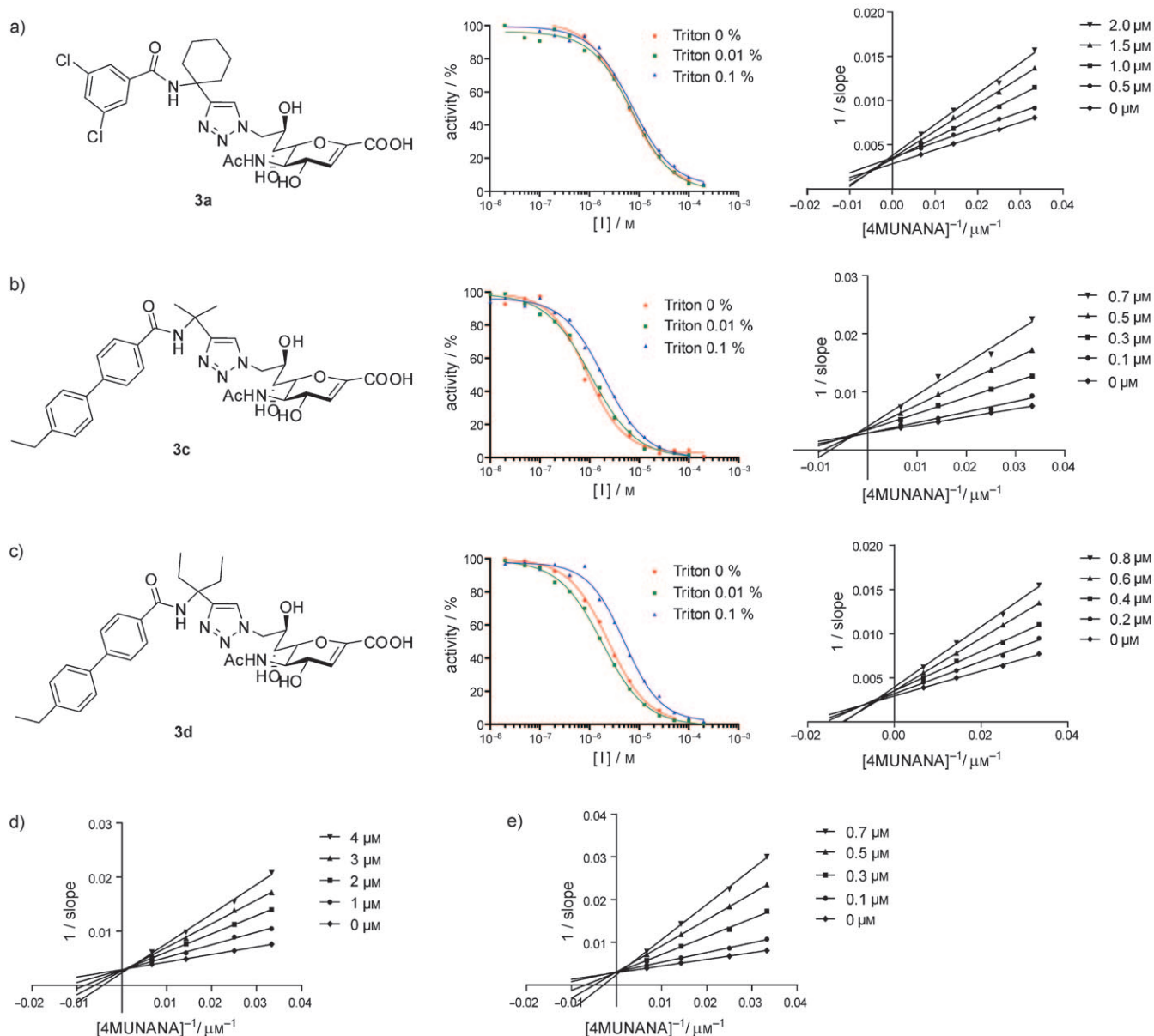


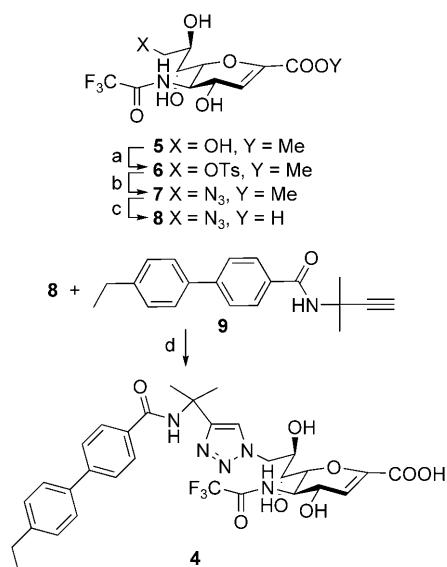
Figure 3. Structure, sigmoid curve profile of detergent-dependent identification, and LB plot of a) **3a**, b) **3c**, and c) **3d**, and LB plot of d) DANA and e) FANA.

compound with both substituted groups, **4**, can be a more potent inhibitor for VCNA along with a high selectivity like **3c**. Compound **4** was prepared from the methyl ester derivative of FANA (**5**)<sup>[10]</sup> in four steps (Scheme 2). Monotosylation of **5** gave **6**, and this was followed by S<sub>N</sub>2 replacement to give the 9-N<sub>3</sub> derivative **7**. Saponification of the methyl ester group of **7** gave the 9-N<sub>3</sub> analogue of FANA **8** with a 15% overall yield over three steps. Kinetic analysis of **8** by using the LB plot showed that **8** competitively inhibited VCNA with low K<sub>i</sub> values (0.37 μM); the 9-N<sub>3</sub> substitution of **8** did not affect the inhibition property of FANA. The same tendency was observed with the introduction of an azide group at the C9 atom of DANA. The click reaction of **8** with alkyne **9** gave **4** in 70% yield. An inhibition assay

showed that **4** has the lowest K<sub>i</sub> value for VCNA (73 nM) among the reported compounds<sup>[10,11]</sup> with a high selectivity (Figure 4). The mixed inhibition mode and high selectivity among the three NAs means that **4** maintains the inhibition character of **3c**. Although, the substitution effect decreased relative to the change from DANA to FANA and **2** to **8**, the trifluoroacetyl group afforded additional interaction potency to **3c** as expected.

## Conclusion

Protein dynamism, which is difficult to detect by means of current methodologies, can be a potential target for the de-



Scheme 2. Preparation of **4**. Reagents: a) TsCl, pyridine, 0°C, 24 h, 40%; b) NaN<sub>3</sub>, DMF, 70°C, 6 h, 68%; c) NaOH, H<sub>2</sub>O, RT, 20 min, 66%; d) tris(benzyltriazolylmethyl)amine (TBTA), ascorbate, CuSO<sub>4</sub>, H<sub>2</sub>O, *t*BuOH, DMSO, 1 d, 70%.

development of a potent and selective inhibitor. Mechanism-based labeling can be a versatile complement to current drug designs based on the X-ray crystallographic structure of the target proteins. In the case of neuraminidases, it was anticipated that the structural change in the peripheral loop structure of the catalytic domain can be a potential target of novel drug design; however, a clear and practical approach has not yet been reported. In this study, the unexpected modification of amino acid residues observed in the mechanism-based labeling study revealed the presence of an additional potential target loop and enabled us to design a focused library. A novel lead compound **3c** with a potent and selective inhibition property toward VCNA was found from the focused library. The comparative kinetic study of **3c** and the most potent inhibitor, FANA, revealed the orthogonal effect of modification of each compound from the common DANA skeleton to give the most potent inhibitor of VCNA, **4**. Development of a more potent VCNA inhibitor from this lead compound is ongoing. This two-step approach could afford a new strategy for the drug design of structurally novel anti-influenza drugs and for targeting various infective diseases and could complement conventional structure-based drug design strategies as well as recent fragment-based drug design.<sup>[23]</sup> Recently, we found that a derivative of the suicide substrate **1** inhibits *Trypanosoma cruzi* trans-sialidase (TcTS) to decrease the infection ratio of the protozoa to the host cell, and the labeling moiety was revealed to be another pair of Asp and Arg residues using **1**.<sup>[24]</sup> We also identified flavonoid and anthraquinone derivatives as potential and noncompetitive TcTS inhibitors from a natural product library.<sup>[25]</sup> The development of more potent inhibitors of TcTS using this information is currently in progress.

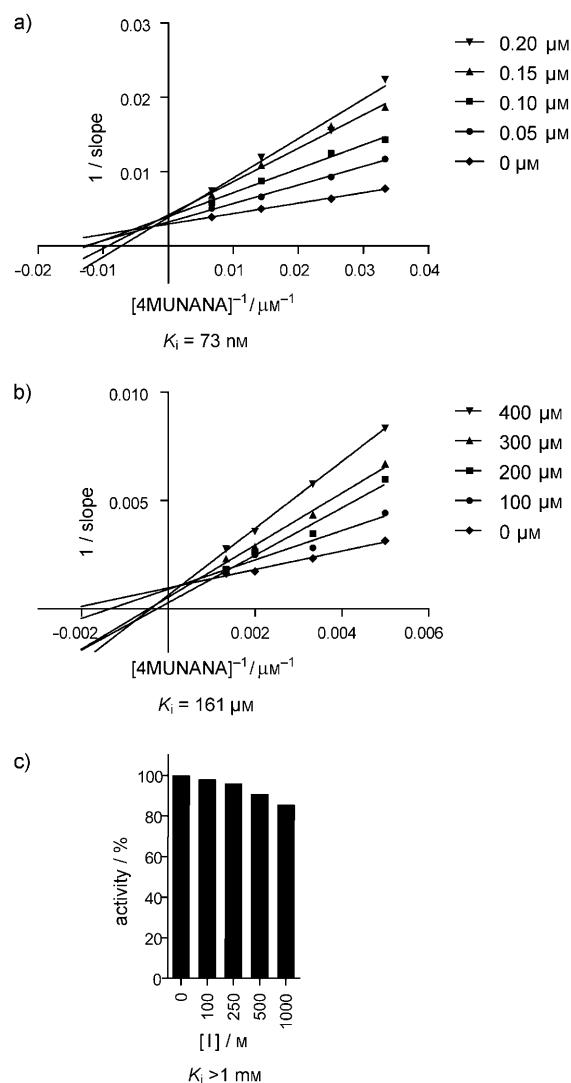


Figure 4. Inhibition property of **4**. LB-plot and  $K_i$  value for a) VCNA and b) *h*Neu2, and inhibition pattern for c) FluB NA.

## Experimental Section

### General

Molecular graphics in Figure 1 were generated and rendered with PyMOL 0.99 software (<http://www.pymol.org>). 2-Deoxy-2,3-dehydro-*N*-acetylneuraminic acid (DANA) and 5-acetamido-2,6-anhydro-9-azido-3,5,9-tri-deoxy-*D*-glycero-*D*-galacto-non-2-enoic acid (**2**), methyl ester of FANA (**5**), and 2- $\alpha$ -(4'-methylumbelliferyl)-*N*-acetylneuraminic acid (4-MU-NANA) were synthesized by following published methods.<sup>[10,26]</sup> Alkyne compounds were purchased from Thermo Fisher Scientific Inc. (230 compounds) and Tokyo Chemical Industry Co., Ltd (36 compounds). *Vibrio cholerae* neuraminidase (lot No. 088K4020) was purchased from Sigma-Aldrich (Japan). Influenza B neuraminidase was donated from SHIONOGI & Co., Ltd. Human neuraminidase 2 was prepared as in a reported procedure.<sup>[12]</sup> The purity (>95%) of each compound was also checked by <sup>1</sup>H NMR spectroscopy (see the Supporting Information). The activity of neuraminidase was measured by fluorescence spectrometry in the presence of 4-MU-NANA as a substrate using a microplate reader (SpectraMax M5, Molecular Devices Co., Sunnyvale, CA). Analyses of assay results were performed by using PRISM software 5.01 (GraphPad Software Inc., San Diego, CA).

## Construction of Compound Libraries for First Screening

A solution of **2** (50 mM), alkyne compounds (50 mM),  $\text{CuSO}_4 \cdot 5\text{H}_2\text{O}$  (2.5 mM), and sodium ascorbate (25 mM) in *tert*-butyl alcohol/ $\text{H}_2\text{O}$  (1:1), and a solution of tris(benzyltriazolylmethyl)amine (TBTA; 2.5 mM) in dimethyl sulfoxide (DMSO) were prepared, respectively. Then aliquots of these solutions (10  $\mu\text{L}$ ) were mixed at room temperature and the mixture was left for 8 h. The yields of triazole products **3** were roughly estimated by comparison of the signal intensity of **2** and each triazole product by ESIMS. The solutions that contained more than 70% yield of the triazole product were used for the following first screening assays of VCNA as 100% yield solutions.

Preparation of **3a**, **3c**, and **3d**

Aliquots (75  $\mu\text{L}$ ) of solutions of **2** (200 mM),  $\text{CuSO}_4 \cdot 5\text{H}_2\text{O}$  (10 mM), sodium ascorbate (100 mM), and alkyne compound (200 mM) in *tert*-butyl alcohol/ $\text{H}_2\text{O}$  (1:1), and of TBTA (10 mM) in DMSO were mixed at room temperature and the mixtures were shaken on a vortex mixer overnight. After checking the completion of the reactions by ESIMS, each reaction mixture was purified by reversed phase (RP) HPLC to give **3a** (31%), **3c** (40%), and **3d** (48%), respectively.

5-Acetamido-2,6-anhydro-9-[4-[(3,5-dichlorobenzamido)cyclohexyl]-1H-1,2,3-triazol-1-yl]-3,5,9-trideoxy-D-glycero-D-galactonon-2-enoic acid (**3a**)

$^1\text{H}$  NMR (600 MHz,  $\text{CD}_3\text{OD}$ ):  $\delta$  = 7.92–7.62 (m, 4H; aromatic), 5.97 (d,  $J$  = 1.8 Hz, 1H; H-3), 4.84 (m, 1H; H-9a), 4.43 (m, 1H; H-4, 9b), 4.27 (ddd,  $J$  = 2.4, 6.6, 9.0 Hz, 1H; H-8), 4.18 (d,  $J$  = 10.8 Hz, 1H; H-6), 4.01 (dd,  $J$  = 9.0, 10.8 Hz, 1H; H-5), 3.46 (d,  $J$  = 9.0 Hz, 1H; H-7), 2.55 (m, 2H), 2.10 (m, 2H), 2.04 (s, 3H; Ac), 1.69–1.44 ppm (m, 6H);  $^{13}\text{C}$  NMR (125 MHz,  $\text{CD}_3\text{OD}$ ):  $\delta$  = 173.62, 138.59, 134.88, 130.57, 125.91, 112.13, 76.42, 70.00, 68.46, 66.50, 53.88, 50.53, 35.10, 34.91, 25.14, 21.62, 21.27 ppm; HRMS (FAB-MS):  $m/z$  calcd for  $\text{C}_{26}\text{H}_{32}\text{Cl}_2\text{N}_5\text{O}_8$  [ $M+H$ ] $^+$ : 612.1628; found: 612.1626.

5-Acetamido-2,6-anhydro-9-[4-[(4'-ethylbiphen-4-yl)carboxamidoprop-2-yl]-1H-1,2,3-triazol-1-yl]-3,5,9-trideoxy-D-glycero-D-galactonon-2-enoic acid (**3c**)

$^1\text{H}$  NMR (600 MHz,  $\text{CD}_3\text{OD}$ ):  $\delta$  = 7.92–7.30 (m, 9H; aromatic), 5.97 (d,  $J$  = 2.4 Hz, 1H; H-3), 4.85 (m, 1H; H-9a), 4.43 (m, 2H; H-4, 9b), 4.29 (ddd,  $J$  = 2.4, 6.6, 9.0 Hz, 1H; H-8), 4.19 (dd,  $J$  = 1.2, 10.8 Hz, 1H; H-6), 4.01 (dd,  $J$  = 8.4, 10.8 Hz, 1H; H-5), 3.48 (dd,  $J$  = 1.2, 9.0 Hz, 1H; H-7), 2.70 (q,  $J$  = 7.8 Hz, 2H;  $\text{CH}_2$ ), 2.05 (s, 3H; Ac), 1.84 (m, 6H;  $\text{CH}_3 \times 2$ ), 1.28 ppm (t,  $J$  = 7.8 Hz, 1H;  $\text{CH}_2\text{CH}_3$ );  $^{13}\text{C}$  NMR (125 MHz,  $\text{CD}_3\text{OD}$ ):  $\delta$  = 173.78, 144.18, 137.26, 133.41, 128.40, 128.10, 127.64, 126.64, 126.26, 122.46, 112.11, 76.41, 69.97, 68.50, 66.52, 54.03, 50.53, 28.10, 27.05, 21.27, 14.67 ppm; HRMS (FAB-MS):  $m/z$  calcd for  $\text{C}_{31}\text{H}_{36}\text{N}_5\text{O}_8$  [ $M-H$ ] $^-$ : 606.2569; found: 606.2562.

5-Acetamido-2,6-anhydro-9-[4-[(4'-ethylbiphen-4-yl)carboxamino-pent-3-yl]-1H-1,2,3-triazol-1-yl]-3,5,9-trideoxy-D-glycero-D-galactonon-2-enoic acid (**3d**)

$^1\text{H}$  NMR (600 MHz,  $\text{CD}_3\text{OD}$ ):  $\delta$  = 7.96–7.31 (m, 9H; aromatic), 5.98 (d,  $J$  = 2.4 Hz, 1H; H-3), 4.88 (m, 1H; H-9a), 4.48 (dd,  $J$  = 7.8, 14.4 Hz, 1H; H-9b), 4.44 (dd,  $J$  = 2.4, 9.0 Hz, 1H; H-4), 4.30 (ddd,  $J$  = 2.4, 7.8, 9.0 Hz, 1H; H-8), 4.18 (d,  $J$  = 10.8 Hz, 1H; H-6), 4.01 (dd,  $J$  = 9.0, 10.8 Hz, 1H; H-5), 3.47 (d,  $J$  = 9.0 Hz, 1H; H-7), 2.71 (q,  $J$  = 7.8 Hz, 2H;  $\text{Ar-CH}_2\text{CH}_3$ ), 2.28 (m, 4H;  $\text{CH}_2 \times 2$ ), 2.04 (s, 3H; Ac), 1.28 (t,  $J$  = 7.8 Hz, 3H;  $\text{Ar-CH}_2\text{CH}_3$ ), 0.84 ppm (m, 6H;  $\text{CH}_3 \times 2$ );  $^{13}\text{C}$  NMR (125 MHz,  $\text{CD}_3\text{OD}$ ):  $\delta$  = 173.81, 168.08, 164.09, 150.65, 144.21, 143.98, 137.23, 135.39, 133.00, 128.10, 127.50, 126.66, 126.38, 123.31, 112.14, 76.43, 70.00, 68.42, 66.48, 54.09, 50.55, 28.52, 28.52, 28.11, 21.28, 14.68, 6.62 ppm; HRMS (FAB-MS):  $m/z$  calcd for  $\text{C}_{33}\text{H}_{40}\text{N}_5\text{O}_8$  [ $M-H$ ] $^-$ : 634.2882; found: 634.2859.

Methyl 2,6-anhydro-3,5-dideoxy-9-O-tosyl-5-trifluoroacetamido-D-glycero-D-galactonon-2-enonate (**6**)

At  $-10^\circ\text{C}$ , tosyl chloride (251 mg, 1.32 mmol) was added to a solution of methyl 2,6-anhydro-3,5-dideoxy-5-trifluoroacetamido-D-glycero-D-galac-

tonon-2-enonate **5** (184 mg, 0.51 mmol) in pyridine (8 mL) and the mixture was stirred under a nitrogen atmosphere at  $0^\circ\text{C}$  for 24 h. Next, MeOH (2 mL) was added to the mixture, which was then concentrated under vacuum. Purification of the residue on a column of silica gel (4:3 hexane/acetone) afforded compound **6** (105 mg, 40%).  $^1\text{H}$  NMR (500 MHz,  $\text{CD}_3\text{OD}$ ):  $\delta$  = 7.84 (d,  $J$  = 8.3 Hz, 2H; aromatic), 7.47 (d,  $J$  = 8.3 Hz, 2H; aromatic), 5.97 (d,  $J$  = 2.4 Hz, 1H; H-3), 4.52 (dd,  $J$  = 2.4, 8.8 Hz, 1H; H-4), 4.37 (m, 2H; H-6, 9a), 4.17 (dd,  $J$  = 9.0, 10.7 Hz, 1H; H-5), 4.13 (dd,  $J$  = 6.1, 10.0 Hz, 1H; H-9b), 4.07 (ddd,  $J$  = 2.0, 6.1, 8.9 Hz, 1H; H-8), 3.82 (s, 3H;  $\text{COOCH}_3$ ), 3.50 (d,  $J$  = 8.6 Hz, 1H; H-7), 2.48 ppm (s, 3H;  $\text{Ar-CH}_3$ );  $^{13}\text{C}$  NMR (125 MHz,  $\text{CD}_3\text{OD}$ ):  $\delta$  = 162.82, 145.04, 143.48, 132.90, 129.62, 129.49, 127.76, 127.69, 112.35, 75.55, 72.25, 68.28, 67.76, 66.31, 51.50, 50.57, 20.18 ppm; HRMS (FAB):  $m/z$  calcd for  $\text{C}_{19}\text{H}_{21}\text{F}_3\text{NO}_8$  [ $M-H$ ] $^-$ : 512.0844; found: 512.0844.

Methyl 2,6-anhydro-9-azido-3,5,9-trideoxy-5-trifluoroacetamido-D-glycero-D-galactonon-2-enonate (**7**)

Sodium azide (78 mg, 1.2 mmol) was added to a solution of **6** (100 mg, 0.19 mmol) in *N,N*-dimethylformamide (DMF; 1.5 mL) and the mixture was stirred at  $70^\circ\text{C}$ . After 6 h, the reaction mixture was allowed to cool to room temperature. Purification of the mixture on a column of silica gel (2:1 hexane/acetone) afforded compound **7** (50 mg, 68%).  $^1\text{H}$  NMR (500 MHz,  $\text{CD}_3\text{OD}$ ):  $\delta$  = 5.95 (d,  $J$  = 2.4 Hz, 1H; H-3), 4.49 (dd,  $J$  = 2.3, 8.8 Hz, 1H; H-4), 4.40 (d,  $J$  = 10.9 Hz, 1H; H-6), 4.19 (dd,  $J$  = 1.4, 10.6 Hz, 1H; H-5), 4.03 (ddd,  $J$  = 2.5, 6.5, 9.3 Hz, 1H; H-8), 3.79 (s, 3H;  $\text{COOCH}_3$ ), 3.56 (dd,  $J$  = 2.5, 10.8 Hz, 1H; H-9a), 3.49 (d,  $J$  = 9.3 Hz, 1H; H-7), 3.39 ppm (dd,  $J$  = 6.3, 12.8 Hz, 1H; H-9b);  $^{13}\text{C}$  NMR (125 MHz,  $\text{CD}_3\text{OD}$ ):  $\delta$  = 162.90, 143.57, 112.37, 75.69, 69.20, 69.12, 66.46, 54.20, 51.48, 50.60 ppm; HRMS (FAB):  $m/z$  calcd for  $\text{C}_{12}\text{H}_{14}\text{F}_3\text{N}_4\text{O}_7$  [ $M-H$ ] $^-$ : 383.0820; found: 383.0812.

5-Trifluoroacetamido-2,6-anhydro-9-azido-3,5,9-trideoxy-D-glycero-D-galactonon-2-enoic acid (**8**)

NaOH (1 M, 0.1 mL) was added to a solution of **7** (25 mg, 0.07 mmol) in  $\text{H}_2\text{O}$  (1.6 mL) and the mixture was stirred at room temperature for 20 min. The reaction mixture was neutralized by the addition of Dowex 50W  $\times$  8 resin. The mixture was filtered and lyophilized to give compound **8** (16 mg, 66%) as a white solid. The product was used for the following reaction without further purification.  $^1\text{H}$  NMR (500 MHz,  $\text{D}_2\text{O}$ ):  $\delta$  = 5.63 (d,  $J$  = 2.2 Hz, 1H; H-3), 4.47 (dd,  $J$  = 2.2, 8.9 Hz, 1H; H-4), 4.29 (d,  $J$  = 11.0 Hz, 1H; H-6), 4.14 (dd,  $J$  = 9.3, 10.6 Hz, 1H; H-5), 4.03 (ddd,  $J$  = 2.7, 5.8, 9.1 Hz, 1H; H-8), 3.57 (dd,  $J$  = 2.7, 13.2 Hz, 1H; H-9a), 3.50 (d,  $J$  = 9.4 Hz, 1H; H-7), 3.43 ppm (dd,  $J$  = 5.8, 13.1 Hz, 1H; H-9b);  $^{13}\text{C}$  NMR (125 MHz,  $\text{D}_2\text{O}$ ):  $\delta$  = 169.32, 147.88, 107.73, 74.58, 68.63, 68.60, 67.25, 53.66, 50.57 ppm; HRMS (FAB):  $m/z$  calcd for  $\text{C}_{11}\text{H}_{12}\text{F}_3\text{N}_4\text{O}_7$  [ $M-H$ ] $^-$ : 369.0664; found: 369.0652.

2,6-Anhydro-9-[4-[(4'-ethylbiphen-4-yl)carboxamido-prop-2-yl]-1H-1,2,3-triazol-1-yl]-3,5,9-trideoxy-5-trifluoroacetamido-D-glycero-D-galactonon-2-enoic acid (**4**)

Solutions of azido **8** (200 mM),  $\text{CuSO}_4 \cdot 5\text{H}_2\text{O}$  (10 mM), and sodium ascorbate (100 mM) in *tert*-butyl alcohol/ $\text{H}_2\text{O}$  (1:1) and solutions of alkyne **9** (300 mM) and TBTA (10 mM) in DMSO were prepared, respectively. Aliquots (135  $\mu\text{L}$ ) of each solution were mixed at room temperature and left for 24 h. The reaction mixture was purified by HPLC to give **4** (13 mg, 70%) as a white powder after lyophilization.  $^1\text{H}$  NMR (500 MHz,  $(\text{CD}_3)_2\text{CO}$ ):  $\delta$  = 8.69 (d, 1H;  $\text{CF}_3\text{CONHR}$ ), 7.95 (s, 1H;  $\text{N-CH=CRN}$ ), 7.91 (d,  $J$  = 8.3 Hz, 2H; aromatic), 7.82 (s, 1H;  $\text{Ar-CONHR}$ ), 7.71–7.61 (m, 4H; aromatic), 7.33 (d,  $J$  = 8.2 Hz, 2H; aromatic), 5.98 (d,  $J$  = 2.5 Hz, 1H; H-3), 4.91 (dd,  $J$  = 2.3, 14.0 Hz, 1H; H-9a), 4.71 (dd,  $J$  = 2.5, 8.6 Hz, 1H; H-4), 4.54 (d,  $J$  = 10.6 Hz, 1H; H-6), 4.42 (dd,  $J$  = 8.3, 14.0 Hz, 1H; H-9b), 4.31–4.28 (m, 2H; H-5,8), 3.60 (dd,  $J$  = 0.8, 8.9 Hz, 1H; H-7), 2.69 (q,  $J$  = 7.6 Hz, 2H;  $\text{CH}_2\text{CH}_3$ ), 1.85 (s,  $J$  = 7.6 Hz, 6H;  $\text{CH}_3 \times 2$ ), 1.24 ppm (t,  $J$  = 7.6 Hz, 3H;  $\text{CH}_2\text{CH}_3$ );  $^{13}\text{C}$  NMR (125 MHz,  $(\text{CD}_3)_2\text{CO}$ ):  $\delta$  = 165.93, 165.87, 152.97, 144.11, 143.82, 143.46, 137.35, 134.23, 128.42, 127.75, 126.92, 126.38, 122.26, 112.39, 75.65, 70.16, 69.26, 66.26, 53.80, 15.10 ppm; HRMS (FAB):  $m/z$  calcd for  $\text{C}_{31}\text{H}_{33}\text{F}_3\text{N}_5\text{O}_8$  [ $M-H$ ] $^-$ : 660.2287; found: 660.2289.

*VCNA: First and Second Screening*

Each compound of the first and second screening library (100 and 50  $\mu\text{M}$ , respectively) was incubated with 4 mM  $\text{CaCl}_2$ , VCNA, and 4-MU-NANA in sodium acetate buffer (100 mM, pH 6.5) at 37 °C for 5 min. The relative inhibition ratios of VCNA by the first and second screening library were estimated by using a microplate reader at excitation and emission wavelengths of 365 and 450 nm, respectively.

*Detergent-Based Assays*

The experiments for detergent-based assays were performed by using 150  $\mu\text{M}$  4-MU-NANA concentrations and several concentrations of inhibitor. The assay mixture—containing 4 mM  $\text{CaCl}_2$ , 0, 0.01, or 0.1% Triton X-100, 100  $\mu\text{g mL}^{-1}$  bovine serum albumin (BSA), 0.076 mU VCNA, and inhibitor in 2-(*N*-morpholino)ethanesulfonic acid (MES)/NaOH buffer (33 mM, pH 6.5)—was preincubated for 30 min at 25 °C and the reaction was initiated by addition of 4-MU-NANA in a final volume of 120  $\mu\text{L}$ . After incubation (10, 20, 30, and 40 min), aliquots (20  $\mu\text{L}$ ) of the reaction mixture were taken and the enzymatic reaction was quenched by addition to a 100 mM glycine solution at pH 10.8 (80  $\mu\text{L}$ ) in a 96-well plate. The fluorescence of the released product (4-MU) was measured at 25 °C with excitation and emission wavelengths of 365 and 450 nm, respectively. Each sigmoid curve was derived from a plot of percent activity versus inhibitor concentration.

*Determination of  $K_i$  values*

The experiments for  $K_i$  determination were performed in 30 to 150  $\mu\text{M}$  4-MU-NANA concentrations and several concentrations of inhibitor. The assay mixture—containing 33 mM MES, 4 mM  $\text{CaCl}_2$ , 100  $\mu\text{g mL}^{-1}$  BSA, 0.076 mU VCNA, and inhibitor in MES/NaOH buffer (33 mM, pH 6.5)—was preincubated for 30 min at 25 °C and the reaction was initiated by addition of 4-MU-NANA in a final volume of 120  $\mu\text{L}$ . After incubation (10, 20, 30, and 40 min), aliquots (20  $\mu\text{L}$ ) of the reaction mixture were taken and the enzymatic reaction was quenched by addition to a 100 mM glycine solution at pH 10.8 (80  $\mu\text{L}$ ) in a 96-well plate. The fluorescence of the released product (4-MU) was measured at 25 °C with excitation and emission wavelengths of 365 and 450 nm, respectively. The  $K_i$  value and the competitive nature of the inhibition were determined by Lineweaver–Burk plot analysis.

*FluB NA*

The experiments for  $K_i$  determination were performed in 8 to 30  $\mu\text{M}$  4-MU-NANA concentrations and several concentrations of inhibitor. The assay mixture—containing 4 mM  $\text{CaCl}_2$ , 0.067 mU Influenza B, and inhibitor in MES/NaOH buffer (33 mM, pH 6.5)—was preincubated for 30 min at 25 °C and reaction was initiated by addition of 4-MU-NANA in a final volume of 120  $\mu\text{L}$  at 37 °C. After incubation (10, 20, 30, and 40 min), aliquots (20  $\mu\text{L}$ ) of the reaction mixture were taken and the enzymatic reaction was quenched by addition to a 100 mM glycine solution at pH 10.8 (80  $\mu\text{L}$ ) in a 96-well plate. The fluorescence of the released product (4-MU) was measured at 25 °C with excitation and emission wavelengths of 365 and 450 nm, respectively. The  $K_i$  value and the competitive nature of the inhibition were determined by Lineweaver–Burk plot analysis.

*Neu2*

The experiments for  $K_i$  determination were performed in 200 to 750  $\mu\text{M}$  4-MU-NANA concentrations and several concentrations of inhibitor. The assay mixture—containing 100 mM Na citrate/phosphate pH 6.5, buffer, 100  $\mu\text{g mL}^{-1}$  BSA, 0.30 mU Neu2, and inhibitor solution—was preincubated for 30 min at 25 °C and the reaction was initiated by addition of 4-MU-NANA in a final volume of 120  $\mu\text{L}$  at 37 °C. After incubation (10, 20, 30, and 40 min), aliquots (20  $\mu\text{L}$ ) of the reaction mixture were taken and the enzymatic reaction was quenched by addition to a 100 mM glycine solution at pH 10.8 (80  $\mu\text{L}$ ) in a 96-well plate. The fluorescence of the released product (4-MU) was measured at 25 °C with excitation and emission wavelengths of 365 and 450 nm, respectively. The  $K_i$  value and the competitive nature of the inhibition were determined by Lineweaver–Burk plot analysis.

**Acknowledgements**

This work was supported by funding from the Ministry of Education, Culture, Science, Sports and Technology of Japan for “Grant-in-Aid for Young Scientists (A)” and “Innovation COE Program for Future Drug Discovery and Medical Care”. We thank Ms. M. Kikuchi, Ms. S. Oka, and Mr. T. Hirose at the Center for Instrumental Analysis, Hokkaido University, for ESIMS measurements.

- a) T. Angata, A. Varki, *Chem. Rev.* **2002**, *102*, 439–469; b) A. Varki, *Nature* **2007**, *446*, 1023–1029.
- E. Severi, D. W. Hood, G. H. Thomas, *Microbiology* **2007**, *153*, 2817–2822.
- A. Gottschalk, *Biochim. Biophys. Acta* **1957**, *23*, 645–646.
- J. E. Galen, J. M. Ketley, A. Fasano, S. W. Richardson, S. S. Wasserman, J. B. Kaper, *Infect. Immun.* **1992**, *60*, 406–415.
- S. Almagro-Moreno, E. F. Boyd, *Infect. Immun.* **2009**, *77*, 3807–3816.
- S. Crennell, E. Garman, G. Laver, E. Vimr, G. Taylor, *Structure* **1994**, *2*, 535–544.
- M. von Itzstein, *Curr. Opin. Struct. Biol.* **2008**, *18*, 558–566.
- M. von Itzstein, W. Y. Wu, G. B. Kok, M. S. Pegg, J. C. Dyason, B. Jin, T. Van Phan, M. L. Smythe, H. F. White, S. W. Oliver, P. M. Colman, J. N. Varghese, D. M. Ryan, J. M. Woods, R. C. Bethell, V. J. Hotham, J. M. Cameron, C. R. Penn, *Nature* **1993**, *363*, 418–423.
- C. U. Kim, W. Lew, M. A. Williams, H. T. Liu, L. J. Zhang, S. Swaminathan, N. Bischofberger, M. S. Chen, D. B. Mendel, C. Y. Tai, W. G. Laver, R. C. Stevens, *J. Am. Chem. Soc.* **1997**, *119*, 681–690.
- D. Meindl, G. Bodo, P. Palese, J. Schulman, H. Tuppy, *Virology* **1974**, *58*, 457–463.
- a) P. Florio, R. J. Thomson, A. Alafaci, S. Abo, M. von Itzstein, *Bioorg. Med. Chem. Lett.* **1999**, *9*, 2065–2068; b) J. C. Wilson, R. J. Thomson, J. C. Dyason, P. Florio, K. J. Quelch, S. Abo, M. von Itzstein, *Tetrahedron: Asymmetry* **2000**, *11*, 53–73; c) H. Streicher, C. Bohner, *Tetrahedron* **2002**, *58*, 7573–7581; d) M. C. Mann, R. J. Thomson, M. von Itzstein, *Bioorg. Med. Chem. Lett.* **2004**, *14*, 5555–5558; e) M. C. Mann, R. J. Thomson, J. C. Dyason, S. McAtamney, M. von Itzstein, *Bioorg. Med. Chem.* **2006**, *14*, 1518–1537; f) H. Streicher, H. Busse, *Bioorg. Med. Chem.* **2006**, *14*, 1047–1057.
- L. M. G. Chavas, C. Tringali, P. Fusi, B. Venerando, G. Tettamanti, R. Kato, E. Monti, S. Wakatsuki, *J. Biol. Chem.* **2005**, *280*, 469–475.
- R. J. Russell, L. F. Haire, D. J. Stevens, P. J. Collins, Y. P. Lin, M. Blackburn, A. J. Hay, S. J. Gamblin, J. J. Skehel, *Nature* **2006**, *443*, 45–49.
- W.-H. Wen, S.-Y. Wang, K.-C. Tsai, Y.-S. E. Cheng, A.-S. Yang, J.-M. Fang, C.-H. Wong, *Bioorg. Med. Chem.* **2010**, *18*, 4074–4084.
- H. Hinou, S.-I. Nishimura, *Curr. Top. Med. Chem.* **2009**, *9*, 106–116.
- S. Halazy, V. Berges, A. Ehrhard, C. Danzin, *Bioorg. Chem.* **1990**, *18*, 330–344.
- H. Hinou, M. Kuroguchi, H. Shimizu, S.-I. Nishimura, *Biochemistry* **2005**, *44*, 11669–11675.
- I. Moustafa, H. Connaris, M. Taylor, V. Zaitsev, J. C. Wilson, J. M. Kiefel, M. von Itzstein, G. Taylor, *J. Biol. Chem.* **2004**, *279*, 40819–40826.
- H. C. Kolb, M. G. Finn, K. B. Sharpless, *Angew. Chem.* **2001**, *113*, 2056–2075; *Angew. Chem. Int. Ed.* **2001**, *40*, 2004–2021.
- T. G. Warner, A. Louie, M. Potier, A. Ribeiro, *Carbohydr. Res.* **1991**, *215*, 315–321.
- B. Y. Feng, A. Shelat, T. N. Doman, R. K. Guy, B. K. Shoichet, *Nat. Chem. Biol.* **2005**, *1*, 146–148.
- B. Y. Feng, B. K. Shoichet, *Nat. Protoc.* **2006**, *1*, 550–553.
- a) S. H. Rotstein, M. A. Murcko, *J. Med. Chem.* **1993**, *36*, 1700–1710; b) P. J. Hajduk, J. Greer, *Nat. Rev. Drug Discovery* **2007**, *6*, 211–219.
- S. T. Carvalho, M. Sola-Penna, I. A. Oliveira, S. Pita, A. S. Gonçalves, B. C. Neves, F. R. Sousa, L. Freire-de-Lima, M. Kuroguchi,

- H. Hinou, S.-I. Nishimura, L. Mendonça-Previato, J. O. Previato, A. R. Todeschini, *Glycobiology* **2010**, *20*, 1034–1045.
- [25] S. Arioka, M. Sakagami, R. Uematsu, H. Yamaguchi, H. Togame, H. Takemoto, H. Hinou, S.-I. Nishimura, *Bioorg. Med. Chem.* **2010**, *18*, 1633–1640.
- [26] a) H. Kamei, Y. Kajihara, Y. Nishi, *Carbohydr. Res.* **1999**, *315*, 243–250; b) R. W. Myers, R. T. Lee, Y. C. Lee, G. H. Thomas, L. W. Reynolds, Y. Uchida, *Anal. Biochem.* **1980**, *101*, 166–174; c) T. G. Warner, J. S. O'Brien, *Biochemistry* **1979**, *18*, 2783–2787.

Received: August 20, 2010

Published online: February 8, 2011